HIGH-RESOLUTION SATELLITE IMAGE TRIFOCAL TENSOR SOLUTION

Shuang Yang[1], Hongbo Pan [1]*, Tao Huang[1]

[1] School of Geosciences and Info-Physics, Central South University, #932 Lunan Road, Changsha, Hunan Province 410083, PR China

KEY WORDS: Trifocal tensor, Affine camera, Three-view images, High-resolution satellite, Minimal parameterization.

ABSTRACT:

This study presents an efficient algorithm for solving the affine trifocal tensor problem in high-resolution satellite imagery. Because the imaging mode of high-resolution satellites is usually a line-center projection and the field of view is small, it can be approximated as an affine camera for orientation. However, the nature of high-resolution satellite trifocal tensors has not been effectively studied or discussed. To address the shortcomings of the current trifocal tensor direct linear algorithm, this study proposes a minimally parameterized trifocal calculation method that can stably calculate the affine trifocal tensors of high-resolution satellites. Efficacy was demonstrated using ZY3-02 and Pleiades-Neo data.

1. INTRODUCTION

High-resolution satellite images (HRSIs) are important data sources for geographic information systems. Compared to frame images, HRSIs generally have a long focal length and small field of view (FoV); the camera is operated on a satellite platform and exhibits a stable trajectory. Push-broom cameras are major payloads for HRSIs, resulting in a linear central projection. In photogrammetry, a rigorous geometric imaging model is typically used to describe the satellite imaging process. However, the rigorous geometric models differ for different satellites. Therefore, general geometric models, such as rational functions and affine models, were developed for image orientation.

The affine model describes a parallel projection between two-dimensional images and three-dimensional (3D) object space. Owing to the significantly small FoV, the affine model was successfully used for image orientation and error analysis of the HRSIs. The epipolar geometry of HRSIs was studied by Ono. However, the geometric relationship of the three satellite images was not sufficiently focused on; the "triple stereo" images were acquired by three-linear cameras and agile satellites.

Trifocal tensors are well-studied objects in computer vision. The role of the trifocal tensor in the three views is similar to that of the fundamental matrix in the two views, and it includes all the geometric relationships among the three views that do not depend on the scene structure. Thus, the trifocal tensor provides a tool for determining the relative orientation of the three images without requiring approximations. Calculating the trifocal tensor of a three-view image is crucial in exploring the geometric relationship between the three-view images and further to establish spatial constraints between them. Currently, the research on trifocal tensors in the field of computer vision primarily focuses on perspective cameras. The appearance of the trifocal tensor can be traced back to Spetsakis, in which the camera was calibrated, and the trifocal tensor was used to recover the scene structure through straight lines. Hartley later

noted that a trifocal tensor also works when a camera is not calibrated. Shashua first mentioned that the corresponding three points with the same name on the three images satisfied a certain algebraic relationship. Hartley proved that the trilinear relationship coefficient obtained by Shashua is consistent with the elements of a trifocal tensor, which can be calculated from points and lines with the same name. The true tensor representation of the trifocal tensor is given by Triggs: These scholars were committed to the research on robust algorithms and applications with the perspective of three-view tensors. The affine trifocal tensor was first defined as Torr. In the simple case of an affine camera, the necessary and sufficient constraints on the trifocal tensor are provided along with a simple geometric interpretation. However, the affine trifocal tensor has only been discussed as an approximation of the perspective camera-trifocal tensor in the field of computer vision and has not been further studied or discussed, and the corresponding affine trifocal relationship has not yet been fully revealed.

One existing problem is that the affine camera itself is a locally approximated model. For remote sensing images that are used for large-scale maps and require high precision, an approximation method using an affine camera model can meet these requirements. Further, the affine trifocal tensor of satellite images has not been fully discussed and analyzed, and problems remain in using affine cameras to study the solution of satellite image trifocal tensors.

The remainder of this study is organized as follows: Section 2 proposes a derivation method for the affine trifocal tensor and a verification method for solution-thinking accuracy. Section 3 introduces the three algorithms for affine trifocal tensors. Section 4 presents experiments using data from two different satellites to verify the accuracy of the algorithm. Finally, Section 5 concludes this study.

2. AFFINE TRIFOCAL TENSOR ESTIMATION FOR SATELLITE IMAGERY

---

* Corresponding author

The key idea in deriving an affine trifocal tensor is to transform the generic triplet of the affine cameras into a new triplet of tensors that can be used for computation by applying an appropriate 3D homography. This approach can also be used to derive affine fundamental matrices. This process implies that the affine trifocal tensor naturally inherits the stability and reliability of an affine camera.

2.1 Affine Trifocal Tensor Derivation

Let the camera matrices of the three views be $P = [I \mid 0], P' = [A \mid a_4], P'' = [B \mid b_4]$, respectively. A and B are 3×3 matrices, and a_i and b_i are $i(i = 1,...,4)$ columns corresponding to the cameras. In this situation, $T_i = a_i b_4^T - a_4 b_i^T$. The affine camera matrix form replaces the $[I \mid 0]$ of finite camera with the $\begin{bmatrix} 1 & 0 & 0 & 0 \\ 0 & 1 & 0 & 0 \\ 0 & 0 & 0 & 1 \end{bmatrix}$. Consider the camera matrices P_1' and P_2', which are transformed by P_1 and P_2 through the 3D homography matrix H.

$$P_1' = \begin{bmatrix} 1 & 0 & 0 & 0 \\ 0 & 1 & 0 & 0 \\ 0 & 0 & 0 & 1 \end{bmatrix}, P_2' = \begin{bmatrix} a_{11} & a_{12} & a_{14} & a_{13} \\ a_{21} & a_{22} & a_{24} & a_{23} \\ 0 & 0 & 0 & a_{33} \end{bmatrix} \tag{1}$$

$$P_1 = \begin{bmatrix} 1 & 0 & 0 & 0 \\ 0 & 1 & 0 & 0 \\ 0 & 0 & 1 & 0 \end{bmatrix}, P_2 = \begin{bmatrix} a_{11} & a_{12} & a_{13} & a_{14} \\ a_{21} & a_{22} & a_{23} & a_{24} \\ 0 & 0 & a_{33} & 0 \end{bmatrix} \tag{2}$$

$$H = \begin{bmatrix} 1 & 0 & 0 & 0 \\ 0 & 1 & 0 & 0 \\ 0 & 0 & 0 & 1 \\ 0 & 0 & 1 & 0 \end{bmatrix} \tag{3}$$

The fundamental matrix remains the same for the 3Dhomography transformation of each camera; therefore, the fundamental matrix F is the same for both camera pairs:

$$F = \begin{bmatrix} 0 & 0 & -a_{24}a_{33} \\ 0 & 0 & -a_{14}a_{33} \\ a_{24}a_{11} + a_{14}a_{21} & a_{24}a_{12} + a_{14}a_{22} & a_{24}a_{13} + a_{14}a_{23} \end{bmatrix} \tag{4}$$

Extending this method to trifocal tensor calculations:

$$P_3' = \begin{bmatrix} b_{11} & b_{12} & b_{14} & b_{13} \\ b_{21} & b_{22} & b_{24} & b_{23} \\ 0 & 0 & 0 & b_{33} \end{bmatrix} \tag{5}$$

We get:

$$T_1 = \begin{bmatrix} a_{11}b_{14} - a_{14}b_{11} & a_{11}b_{24} - a_{14}b_{21} & 0 \\ a_{21}b_{14} - a_{24}b_{11} & a_{21}b_{24} - a_{24}b_{21} & 0 \\ 0 & 0 & 0 \end{bmatrix}$$

$$T_2 = \begin{bmatrix} a_{12}b_{14} - a_{14}b_{12} & a_{12}b_{24} - a_{14}b_{22} & 0 \\ a_{22}b_{14} - a_{24}b_{12} & a_{22}b_{24} - a_{24}b_{22} & 0 \\ 0 & 0 & 0 \end{bmatrix} \tag{6}$$

$$T_3 = \begin{bmatrix} a_{13}b_{14} - a_{14}b_{13} & a_{13}b_{24} - a_{14}b_{23} & -a_{14}b_{33} \\ a_{23}b_{14} - a_{24}b_{13} & a_{23}b_{24} - a_{24}b_{23} & -a_{24}b_{33} \\ a_{33}b_{14} & a_{33}b_{24} & 0 \end{bmatrix}$$

2.2 Solving Process

First, to extract the connection points, it is necessary to match the images in pairs to obtain the connection points, and then string the connection points together to obtain the required points. After SIFT matching, the initial corresponding relationship of the feature matching is obtained. The initial value of the affine model for image grayscale information matching is accurately initialized using the position and orientation information in the feature descriptor. The affine transformation parameters and radiation correction values were iteratively solved based on the minimum absolute value of the gray difference of the corresponding pixels in the matching window, which reduces the influence of noise in the window on the solution. Finally, a refined point of successful convergence is obtained. By substituting the connection points, the required results can be calculated using three different calculation methods for the trifocal tensor, as described later.

2.3 Accuracy Verification

Recovers the camera matrix from the computed trifocal tensor. The trifocal tensor only expresses the relationship between image elements; hence, it has nothing to do with the 3D projection transformation; therefore, the trifocal tensor can obtain the camera matrix in the meaning of only one projection ambiguity. First, you need to find the antipole: let u_i and v_i be the left and right zero vectors of T_i, respectively, that is, $u_i^T T_i = 0^T$ and $T_i v_i = 0$. The antipole can be obtained by $e'^T [u_1, u_2, u_3] = 0^T$ and $e''^T [v_1, v_2, v_3] = 0^T$. After that, the antipole is normalized to the unit norm. Let $P = [I \mid 0]$, then $P' = [[T_1, T_2, T_3]e'' \mid e']$, and $P'' = [(e''e''^T - I)[T_1^T, T_2^T, T_3^T]e' \mid e'']$. Computes an estimate of object space points according to the triangulation method. There are measurements $x = PX, x' = P'X$ on each image, and these equations can be combined into the form of $DX = 0$, where $D = \begin{bmatrix} xP^{3T} & -P^{1T} \\ yP^{3T} & -P^{2T} \\ x'P'^{3T} & -P'^{1T} \\ y'P'^{3T} & -P'^{2T} \end{bmatrix}$. The coordinates of the object space point can be obtained by obtaining X through SVD decomposition. Reproject the object space point to the image space by $\tilde{x} = PX, \tilde{x}' = P'X, \tilde{x}'' = P''X$, and evaluate the error with the original image space point.

3. CALCULATION METHOD

3.1 Affine Minimal Parameterization

The aim is to determine an optimal solution of the affine trifocal tensor between the three views, given three sets of image-matching points. The algorithm proposed in this study indirectly addresses the internal constraints by computing the existence of a minimal parameterization of the affine trifocal tensor. Nordberg describes a minimal set of 18 parameters that can represent any trifocal tensor and its orthogonal matrix, consistent with the internal constraints. The nine parameters describe the three orthogonal matrices and the other nine parameters describe the 10 elements of the sparse tensor T, 17 of which are equal to zero at well-defined positions. Any valid

trifocal tensor was given as a specific tensor transformed by an orthogonal matrix in the corresponding image domain. Describes a simple method for estimating three orthogonal matrices in the general case of $3 \times 3 \times 3$ tensors. This can be used to obtain a least-squares approximation of the general tensors to the tensors satisfying the internal constraints. Conversely, this type of constraint enforcement can be used to obtain improved estimates of trifocal tensors based on a normalized linear algorithm, with constraint enforcement being the last step.

The three camera matrices are defined as:

$$P_1 = (I \mid 0), \quad P_2 = (A \mid a_4), \quad P_3 = (B \mid b_4) \qquad (7)$$

The three transformation matrices are defined as:

$$U_0 = \left(A^{-1}a_4, \left[A^{-1}a_4 \right]_{\times}^2 B^{-1}b_4, \left[A^{-1}a_4 \right]_{\times} B^{-1}b_4 \right)$$

$$V_0 = \left(a_4, [a_4]_{\times} AB^{-1}b_4, [a_4]_{\times}^2 AB^{-1}b_4 \right) \qquad (8)$$

$$W_0 = \left(b_4, [b_4]_{\times} BA^{-1}a_4, [b_4]_{\times}^2 BA^{-1}a_4 \right)$$

To simplify the expressions in the following derivations, the last two matrices can be written as

$$V_0 = (a_4, [a_4]_{\times} r, [a_4]_{\times} r'$$
$$W_0 = (b_4, [b_4]_{\times} s, [b_4]_{\times} s' \qquad (9)$$

where $r = AB^{-1}b_4$, $r' = [a_4]_{\times} r$, $s = BA^{-1}a_4$, $s' = [b_4]_{\times} s$. The three matrices in U_0, V_0, W_0 have orthogonal columns that can be verified based on the nature of the cross-product operator. This implies that proper scaling of each column of these three matrices results in three orthogonal matrices:

$$U = U_0 (U_0^T U_0)^{-\frac{1}{2}}$$

$$V = V_0 (V_0^T V_0)^{-\frac{1}{2}} \qquad (10)$$

$$W = W_0 (W_0^T W_0)^{-\frac{1}{2}}$$

T can be transformed into $\tilde{T}_i'^{jk} = T_m'^{pq} U_p^m V_p^j W_q^k$ by following this rule, which means that each element of $\tilde{T}'$ is obtained by multiplying the triplet of the columns of each U, V, W by the elements of T'.

3.2 Direct Linear Algorithm

Based on the point-point-point correspondence property of the trifocal tensor, in the case of no mismatch, every pair of matching points satisfies $[x']_{\times} \left(\sum_i x^i T_i \right) [x'']_{\times} = 0_{3\times3}$.

$$T = \begin{bmatrix} T_1 & T_2 & T_3 \end{bmatrix} = \begin{bmatrix} t_1 & t_2 & t_3 t_{10} & t_{11} & t_{12} t_{19} & t_{20} & t_{21} \\ t_4 & t_5 & t_6 t_{13} & t_{14} & t_{15} t_{22} & t_{23} & t_{24} \\ t_7 & t_8 & t_9 t_{16} & t_{17} & t_{18} t_{25} & t_{26} & t_{27} \end{bmatrix} \qquad (11)$$

Based on this, $A_{4\times27} t_{27\times1} = 0_{4\times1}$ can be obtained by expanding the formula. It can be seen that at least seven matching point coordinates should be known to obtain t. When there are $m(m \geq 7)$ matching points, the t value can be obtained using singular value decomposition. This method is based on a perspective camera model.

3.3 Affine Direct Linear Method

The first step is similar to that of the direct linear algorithm. According to the properties of the affine trifocal tensor, it can be known that $t_3, t_6, t_7, t_8, t_9, t_{12}, t_{15}, t_{16}, t_{17}, t_{18}, t_{27}$ are all zero. Based

on this, $A_{4\times16} t_{16\times1} = 0_{4\times1}$ can be obtained by expanding the formula.

It can be seen that at least four coordinates of the matching points should be known to obtain t. When there are $m(m \geq 4)$ matching points, the t value can be obtained using singular value decomposition.

The trifocal tensor obtained by the direct linear method may contain errors; therefore, it should be corrected for the algebraic error minimum. When the antipoles $e' = a_4$ and $e'' = b_4$ of the first image relative to the other two images are known, the trifocal tensor can be expressed linearly in terms of the remaining elements of the camera matrix, and this relationship can be written linearly as $t = Ea$. Where E is a matrix of 16×18 that represents the linear relationship $T_i = a_i e_4''^T - e_4' b_i^T$ of the elements that are not zero among the 27 elements, a represents the element vector of a_i and b_i, and t is a vector composed of nonzero elements of the trifocal tensor. The minimization problem is transformed by minimizing the algebraic error $\|AEa\|$ to satisfy $\|Ea\| = 1$.

The algorithm is implemented as follows. Calculate the singular value of E, that is, $E = UDV^T$. Then, the singular value AU, that is, $AU = U'D'V'^T$. Finally, an $t = UV'$ is required.

4. EXPERIMENTS

4.1 Experimental Data

The experimental data adopted were the ZY3-02 and Pleiades satellite. ZY3-02 is a high-resolution stereo mapping service satellite equipped with payloads, such as a three-line array mapping camera and a multispectral camera; the front and rear cameras have a resolution of 2.1 meters.

The experimental data for ZY3-02 were obtained from satellite image data of Changsha. This area is located in central China and has a complex terrain, including plains and mountainous areas, which can better verify the accuracy of the algorithm. The size of the entire NAD image was $24,513 \times 23,995$ pixels.

The Pleiades Neo satellite is a new-generation 0.3 m optical remote sensing commercial satellite from the French Airbus company consisting of four satellites; the fastest possible daily revisit involved four satellites. It has high resolution, integrated detection, strong image-acquisition capability, high satellite agility, and high-frequency constellation revisiting.

The Pleiades Neo dataset uses data from Marseille, France. Marseille is located in southern France, with rolling hills surrounded by limestone hills on three sides. The south-eastern region is located close to the Mediterranean Sea. Because the original image was too large, an image with a size of $10,000 \times 10,000$ pixels was cropped as a global image for calculation.
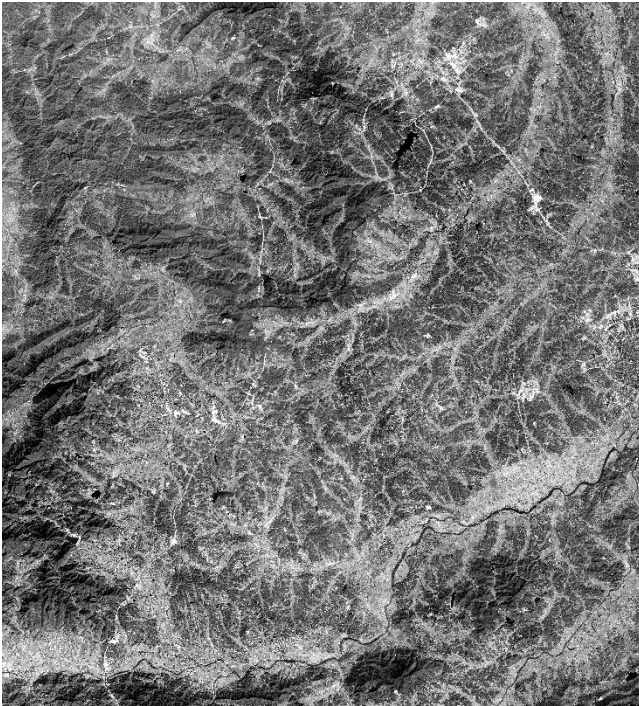
Figure 1. ZY3-02 image of Changsha.
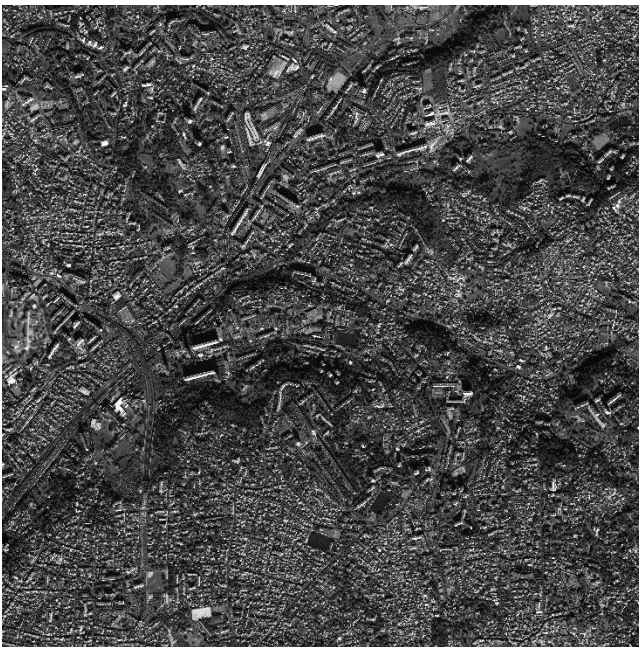
Figure 2. Pleiades neo image of Marseille.

4.2 Experimental Design

First, we verified the accuracy of the trifocal tensor obtained using the three algorithms for a 3,000 × 3,000 pixels image size using different points. For comparison, 10, 100, and 1,000 groups of points were selected. Three sets of projection matrices were obtained using the trifocal tensor, and the reprojection error of the point was calculated for accuracy evaluation.

Point number	Minimizing Algebraic Errors	Minimal Parameterization	Direct Linear Algorithm
10 points	0.43	0.86	0.99
100 points	0.46	0.53	0.56
1000 points	0.49	0.51	0.53

Table 1. RMSE of ZY3-02 image.

Point number	Minimizing Algebraic Errors	Minimal Parameterization	Direct Linear Algorithm
10 points	0.30	0.41	0.37
100 points	0.50	0.59	0.65
1000 points	0.59	0.58	0.64

Table 2. RMSE of Pleiades neo image.

The experimental results show that in the case of fixed-size images, the affine trifocal tensor obtained using 10, 100, and 1,000 groups of points can obtain better results.
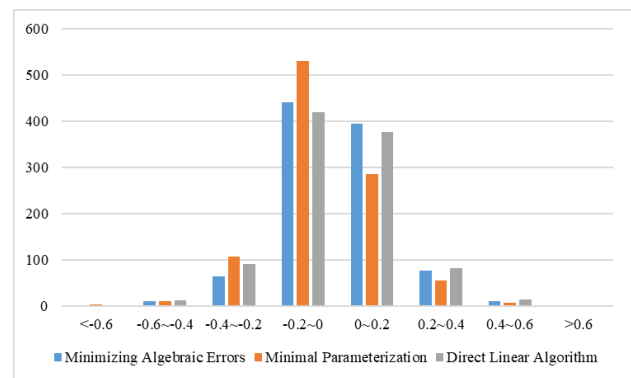
Figure 3. Error distribution of ZY3-02 image.
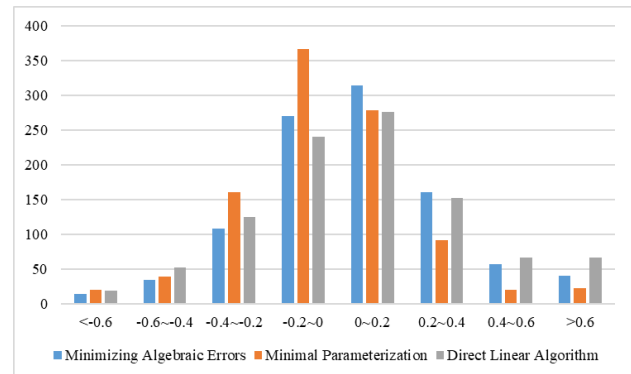
Figure 4. Error distribution of Pleiades neo image.

This part of the experiment verifies the accuracy of the trifocal tensor obtained by the three algorithms for global and local images using the same number of points. To satisfy the statistical principles, 100 groups of points with uniform distributions were randomly selected for the calculation. Three sets of projection matrices were obtained using the trifocal tensor, and the re-projection error of the point was calculated for accuracy evaluation.

Area size	Minimizing algebraic errors	Minimal parameterization	Universal trifocal tensor algorithm
local	0.46	0.53	0.56
global	0.41	0.50	0.66

Table 3. RMSE of ZY3-02 image.

Area size	Minimizing algebraic errors	Minimal parameterization	Universal trifocal tensor algorithm
local	0.45	0.49	0.65
global	0.40	0.41	1.47

Table 4. RMSE of Pleiades neo image.

The experimental results demonstrated the accuracy of the trifocal tensor obtained using 100 sets of points for global and local images. It can be observed that the three algorithms achieved better results for the ZY302 global and local images, and the reprojection errors were small. In the global case, the points can be distributed more evenly; thus, relatively better results can be obtained. However, the direct linear algorithm faces global and local images of Pleiades, and its accuracy is poor. This illustrates the shortcomings of the direct linear algorithm.
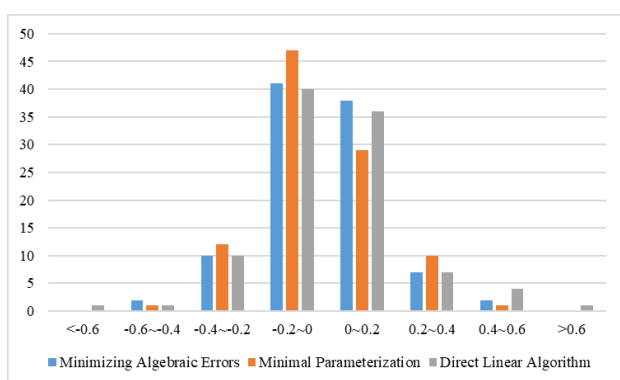
Figure 5. Error distribution of the local image.
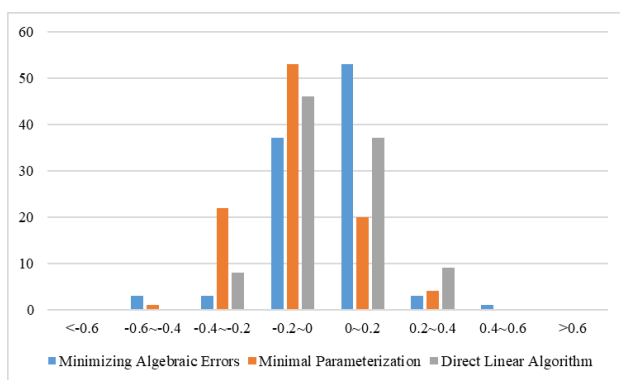
Figure 6. Error distribution of the global image.

Affine models may be less applicable to areas with rougher terrain To explore the problem, the plain and mountainous areas of the same size cropped from the ZY302 satellite image were selected to verify the accuracy of the algorithm in the third part of the experiment.

Point number	Minimizing Algebraic Errors	Minimal Parameterization	Direct Linear Algorithm
10 points	0.43	0.86	0.99
100 points	0.46	0.53	0.56
1000 points	0.49	0.51	0.53

Table 5. RMSE of Plain area.

Point number	Minimizing	Minimal	Direct

	Algebraic Errors	Parameterization	Linear Algorithm
10 points	1.50	0.34	0.37
100 points	0.97	0.52	2.24
1000 points	1.11	0.79	3.71

Table 6. RMSE of Mountains.

Clearly from the experimental results, the affine model has a problem of poor accuracy in rugged mountainous areas, and the accuracy of the three algorithms has declined. However, the affine minimum parameter algorithm shows a relatively good effect, indicating that, after adding the minimum parameterization constraint, the algorithm has a certain universality for terrain undulations.
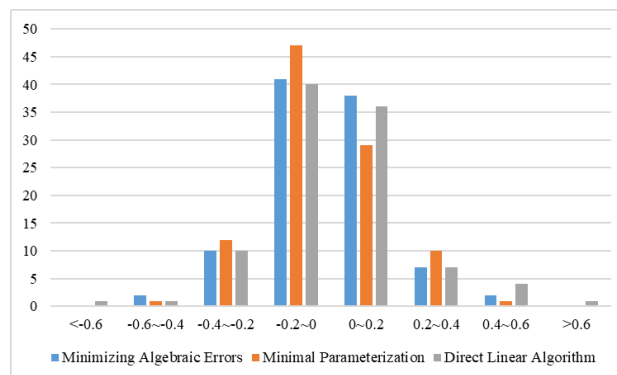
Figure 7. Error distribution of Plain area.
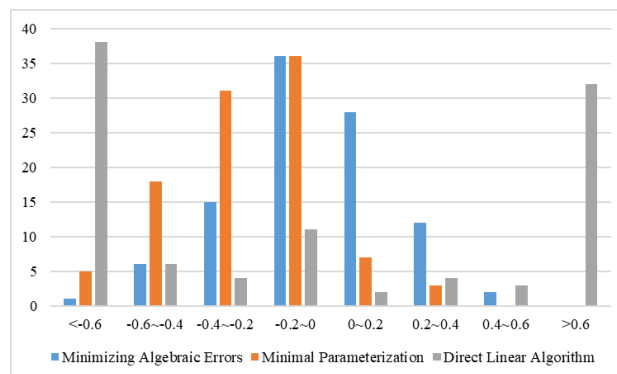
Figure 8. Error distribution of Mountains.

5. CONCLUSION

The imaging mode of high-resolution satellites is usually a line-center projection, and the field of view is small. Therefore, the camera can be approximated as an affine camera. In this study, three different methods were used to compute the affine trifocal tensor of HRSIs to solve the problem of affine three-view geometry on three views.

Affine trifocal tensor can be used to describe the geometry of three HRSIs. Accuracy assessments were performed using different number of points of the same name, different image area ranges, and different types of high-scoring satellites. It can be observed that the minimum parameter method proposed in this study has high accuracy under the same conditions; in addition, it is suitable for different types of high-resolution satellite images, different points, and images of different ranges. In general, direct linear algorithms have relatively poor accuracy on the local and global images and relatively poor

point errors in reprojection. The affine minimum algebraic error and affine minimum parameter methods show little difference in the calculation results of the local and global images, and both can obtain improved results. However, in areas with large terrain fluctuations, the affine minimum parameter algorithm exhibited the best accuracy.

ACKNOWLEDGEMENTS

REFERENCES

Astrom, K., Heyden, A., Kahl, F., & Oskarsson, M. (2002). Structure and motion from lines under affine projections. *Seventh IEEE International Conference on Computer Vision*. IEEE.

Canterakis, N. (2000). A minimal set of constraints for the trifocal tensor. *Proceedings of the 6th European Conference on Computer Vision*, Dublin, Ireland, Springer.

David Nistér. (2004). An efficient solution to the five-point relative pose problem. *IEEE Transactions on Pattern Analysis and Machine Intelligence*.

Fabbri, R., Duff, T., Fan, H., Regan, M., De Pinho, D. D. C., Tsigaridas, E., et al. (2019). Trifocal relative pose from lines at points and its efficient solution.

Fraser, C. S., & Yamakawa, T. (2004). Insights into the affine model for high-resolution satellite sensor orientation. *Isprs Journal of Photogrammetry & Remote Sensing, 58*(5/6), 275-288.

Gugan, D. J., & Dowman, I. J. (1988). Topographic mapping from spot imagery. *Photogrammetric Record, 54*(10), 1409-1414.

Hartley, R. I. (1997). Lines and points in three views and the trifocal tensor. *International Journal of Computer Vision, 22*(2), 125-140.

Hattori, S., Ono, T., Raser, C. F., & Hasegawa, H. (2000). Orientation of high-resolution satellite images based on affine projection.

Hedborg, J., Robinson, A., & Felsberg, M. (2014). Robust Three-View Triangulation Done Fast. *Computer Vision & Pattern Recognition Workshops* (pp.152-157). IEEE.

Kahl, F., & Heyden, A. (1999). Affine structure and motion from points, lines, and conics. *International Journal of Computer Vision, 33*(3), 163-180.

Kamoto, A. (1981). Orientation and construction of models. *Photogrammetric Engineering & Remote Sensing*.

Kanatani, K., Sugaya, Y., & Niitsuma, H. (2008). Triangulation from Two Views Revisited: Hartley-Sturm vs.
Ono, T.. (1999). Epipolar resampling of high-resolution satellite imagery.

Optimal Correction. *Proceedings of the British Machine Vision Conference 2008, Leeds, September 2008.* DBLP.

Mundy, J. L., & Theiss, H. (2021). Error propagation in satellite multi-image geometry.

Mundy, J.L. & Zisserman, A. (Eds). (1992). *Geometric Invariance in Computer Vision*. MIT Press, Cambridge Ma, USA.

Nordberg, K. (2009). A minimal parameterization of the trifocal tensor. *IEEE Conference on Computer Vision & Pattern Recognition*. IEEE.

Papadopoulo, T., & Faugeras, O. (1998). A new characterization of the trifocal tensor. *Proceedings of the 5th European Conference on Computer Vision*, edited by H. Burkhardt and B. Neumann, Springer.

Quan, L. & Kanade, T. (1997). Affine structure from line correspondences with uncalibrated affine cameras. *IEEE Transactions on Pattern Analysis & Machine Intelligence*.

Ressl, C. (2003). Geometry, Constraints, and Computation of the Trifocal Tensor.

Shashua, A., & Werman, M. (1995). On the trilinear tensor of three perspective views and its underlying geometry. *Proceedings of the International Conference on Computer Vision*, Boston, MA.

Thorballsson, T., & Murray, D. W. (1999). The tensors of three affine views. *IEEE Computer Society Conference on Computer Vision & Pattern Recognition*. IEEE.

Torr, P. H. S. (1995). Motion segmentation and outlier detection. *No Abstract Available, 237*(1), iii.

Zisserman, A., & Maybank, S. J. (1997). A Case Against Epipolar Geometry. *Springer Berlin Heidelberg* (Vol.825, pp.69-88). Springer Berlin Heidelberg.